Combination of CYP Inhibitor with MEK/ERK Inhibitor Enhances the Inhibitory Effect on ERK in BRAF Mutant Colon Cancer Cells

SUN MIN LIM[1], JEE WON HWANG[2], JOONG BAE AHN[1,2], SOO KYUNG BAE[3], CHAN HEE PARK[2], KI-YEOL KIM[4], SUN YOUNG RHA[1,2], HYUN CHEOL CHUNG[1,2], JAE KYUNG ROH[1,2] and SANG JOON SHIN[1,2,*]

[1]Department of Internal Medicine, [2]Cancer Metastasis Research Center, Yonsei Cancer Center, Yonsei University College of Medicine, Seoul, Republic of Korea; [3]College of Pharmacy, Catholic University, Seoul, Republic of Korea; [4]Oral Cancer Research Institute, Department of Oral and Maxillofacial Surgery, Yonsei University College of Medicine, Seoul, Republic of Korea

Abstract. *Background/Aim: To investigate mechanisms of discrepancy in response to a MEK/ERK inhibitor, U0126, in KRAS- and BRAF-mutant colorectal cancer cells. Materials and Methods: Multiparametric flow cytometry was performed on two colon cancer cell lines, HCT116 and HT29. Cells were treated with U0126, and phospho-specific antibodies were used to monitor ERK signaling. Results: HCT116 and HT29 cells were treated with increasing amounts of U0126. The western blot analysis revealed that by increasing the amount of U0126 resulted in inhibition of phospho-ERK, in HCT116 and to a lesser degree in HT29 cells. Microarray profiling identified CYP1A1 and 1A2 overexpression in HT29 cells and that inhibition of CYP1A1 with α-naphthoflavone and furanfylline restored sensitivity to U0126 in HT29 cells. Conclusion: Combination of a CYP inhibitor with MEK/ERK inhibitor enhances the inhibitory effect on ERK in BRAF-mutant colon cancer cells.*

Genetic alterations in tyrosine kinases have been firmly implicated in tumorigenesis, and systematic efforts are underway to decipher the genetic changes associated with tumor initiation and progression (1). Numerous results of cancer genome characterization have emerged in recent years, building up detailed knowledge of somatic alterations to develop for optimal targeted cancer therapeutics. In a recent study involving exome sequencing, 52.5% of patients with colorectal cancer had genomic alterations that were directly linked to a clinical therapeutic option (2). As high-throughput technologies have been developed to characterize genetic alterations, it is vital to distinguish between driver oncogenes and passenger oncogenes and to determine which genes are more dominant in oncogenic signaling.

Oncogenic mutations that activate downstream signaling pathways often occur in a mutually exclusive fashion in human cancer. However, several co-occurring mutations have been reported. For example, 30% of all PIK3CA mutations were coincident with another oncogenic mutation. *KRAS* was the most common partner oncogene, but *EGFR* and *BRAF* mutations were also observed to co-occur with *PIK3CA* mutations (3, 4). HCT116, a colon cancer cell line, harbors heterozygous G13D *KRAS* mutations and is also heterozygous for *PIK3CA* mutations. Activating mutations in PIK3CA significantly reduce the response to MEK inhibition. Therefore, combination of a PIK3CA inhibitor and MEK inhibitor are necessary to induce apoptosis in HCT116 cells. In fact, recent studies reported that *KRAS*-mutant tumors require dual inhibition of both the MEK and PIK3CA pathways to achieve inhibition of tumor growth (5, 6).

On the contrary, HT29 cells that harbor a *PIK3CA* mutation respond to MEK inhibitor both in *in vitro* and in *in vivo* tumor models (7, 8). The molecular significance and therapeutic implications of co-occurring mutations in the PI3K and RAS pathway are presently unclear. In a recent study, it was found that the proliferation of *BRAF*-mutant cancer cells was strongly inhibited by inhibition of the MEK pathway, whereas many *KRAS*-mutant tumor cells were resistant to MEK/ERK pathway inhibition (9). Although HCT116 and HT29 cells share common downstream signaling effectors, they demonstrate different responses to MEK inhibitors. In this light, targeting the RAF/MEK/ERK pathway with inhibitors may result in heterogeneous responses in different patients and

Correspondence to: Professor Sang Joon Shin, Cancer Metastasis Research Center, Yonsei Cancer Center, Yonsei University College of Medicine. 50 Yonsei-ro, Seodaemun-gu, Seoul, 120-752, Korea. Tel: +82 222288138, Fax: +82 23933653, e-mail: ssj338@yuhs.ac

Key Words: Cell signaling, ERK, U0126, CYP inhibitor, MEK/ERK inhibitor, colorectal cancer, HT29, HCT116.

may not maximize potential benefits of the targeted agents. Therefore, a quantitative analysis to investigate differences in cell proliferation is required in order to effectively use targeted agents in clinical settings.

In addition, resistance to chemotherapeutic drugs represents a significant hindrance to effective treatment. Acquired resistance to the administered treatment includes induction of mutations leading to a resistant phenotype, epigenetic changes and induction of alternative/compensatory signaling pathways. Alterations in drug metabolism can cause *de novo* resistance, although the cancer cells are sensitive to the therapy. Such alterations take place in the liver, in which drug-metabolizing enzymes such as cytochrome *P450* are located in high concentrations. Besides germline single-nucleotide polymorphisms of cytochrome *P450*, genetic variations associated with drug metabolism in cancer cells also cause inter-individual variation in drug effects (10). Therefore, understanding the contribution of various cytochrome P isoforms to the drug metabolism in cancer cell will allow for better design of clinical trials for the anticipation of drug efficacy.

In this study, we investigated mechanisms of discrepancy in response to a MEK/ERK inhibitor in *KRAS*- and *BRAF*-mutant colorectal cancer cells. We also suggest synergistic anticancer effects of combining cytochrome P inhibitors with a MEK/ERK inhibitor, U0126, for new treatment strategies.

Materials and Methods

Cell culture and agents. HCT116 and HT29 cells were from the American Type Culture Collection (Manassas, VA, USA). Cells were maintained at 37˚C and 5% CO_2 in RPMI-1640 media supplemented with 10% heat-inactivated fetal bovine serum and 1% penicillin/streptomycin (all reagents from Lonza, Basel, Switzerland). Cells were seeded at a density of 0.5-1×10^5 cells/ml, transferred into serum-free media, and starved for 16 h prior to stimulation. U0126, a highly selective inhibitor of both MEK1 and MEK2, was purchased from Calbiochem Corp (La Jolla, CA, USA). α-naphtoflavone and furafylline, inhibitors of Cytochrome P450 were purchased from Sigma-Aldrich Korea (Seoul, Korea).

Flow cytometry. Cells were fixed by the addition of 2% paraformaldehyde/phosphate-buffered saline (PBS) at room temperature for 10 min and permeabilized in ice-cold 100% methanol for 30 min at –20˚C. The samples were washed twice with washing buffer {0.5% bovine serum albumin {BSA}/PBS} and stained for 45 min with conjugated phospho-ERK antibody (p-ERK; Alexa Fluor® 488; Santa Cruz Biotechnology, Santa Cruz, CA, USA). All the antibodies were optimized for concentration. Cells were analyzed using a fluorescence-activated cell sorting (FACS) Caliber flow cytometer (BD Biosciences, San Diego, CA, USA). Flow cytometric data were evaluated using the BD CellQuest™ Pro software (BD Biosciences).

Western blots. Cells were lysed in chilled lysis buffer containing dithiothreitol (DTT), phenylmethylsulfonyl fluoride (PMSF), and a protease inhibitor cocktail. The amount of protein in the extracts was measured using the Bio-Rad protein assay kit (Bio Rad Laboratoreis, Hercules, CA, USA). Equal amounts of proteins were loaded and separated on 10% SDS-PAGE and then transferred to a polyvinylidenedifluoride (PVDF) membrane (Millipore®, Billerica, MA, USA). The membranes were blocked for 1 h with blocking buffer (5% skim milk and 0.1% Tween 20 in PBS) at room temperature on a shaker. The membranes were then incubated overnight at 4˚C with the appropriate primary antibody (in 1× PBS with 0.1% Tween 20). The following antibodies were used: anti-p-ERK and anti-ERK; anti-GAPDH (Abcam, Cambridge, UK); horseradish peroxidase-conjugated anti-mouse and anti-rabbit antibody (Jackson ImmunoResearch Laboratories, West Grove, PA, USA). Immunoreactive proteins were visualized using the enhanced chemiluminescence detection system (Amersham®, GE Healthcare, Buckinghamshire, UK).

Immunofluorescence staining. Cells were seeded on four-well chamber slides (Nalgene Nunc International, Naperville, IL, USA) and treated with U0126. After incubation, the cells were washed with cold PBS and fixed with 4% paraformaldehyde at room temperature for 10 min. The cells were then permeabilized and blocked with 0.2% Triton X-100/1% BSA/PBS at room temperature for 1 h with gentle shaking. Appropriately diluted Alexa488-conjugated antibody to p-ERK was applied onto each chamber for 90 min, followed by a wash with PBS. For additional staining of the cytoskeleton, cells were sequentially incubated with diluted rhodamine-conjugated phalloidin (Invitrogen, Carlsbad, CA, USA). The chamber slides were washed using PBS and mounted using Vectashield-DAPI (Vector Laboratories, Inc. Burlingame, CA, USA). Images were captured and analyzed by confocal microscopy (LSM 700; Carl Zeiss, Jena, Germany).

Cell proliferation assay. Cell proliferation was measured by the 3-(4,5-dimenthylthiazol-2-yl)-2,5-diphenyltetrazolium bromide (MTT) dye reduction method. Cancer cells were plated in triplicate in 96-well plates (2×10^3 cells/well) and incubated in minimum essential medium (MEM) containing 5% FBS. HUVECs were plated in 96-well plates pre-coated with 1.5% gelatin (2×10^3 cells/well) and incubated in supplemented M131 medium. After incubating for 24 h, cells were washed and incubated for 72 h with bevacizumab in fresh MEM containing 5% FBS in the presence or absence of VEGF. MTT stock solution (2 mg/ml; Sigma, Saint Louis, MO, USA) were added to each well and the cells were incubated for 2 h at 37˚C. Media were removed, and 100 μl dimethyl sulfoxide was added to dissolve the dark blue crystals. Absorbance was measured with an MTP-120 microplate reader (Corona Electric, Japan) at wavelengths of 550 and 630 nm, respectively.

RNA preparation. The total RNA was extracted from the HT29 and HCT116 colon cancer cell lines using the TRIzol reagent (Invitrogen) according to the manufacturer's instructions. The Yonsei reference RNA (Cancer Metastasis Research Center, Seoul, Korea) was prepared by pooling equivalent amounts of the total RNA from the following 11 human cancer cell lines: YCC-3 (gastric cancer), YCC-B1 (breast cancer), HCT-116 (colon cancer), SK-HEP-1 (liver cancer), A549 (lung cancer), HL-60 (acute promyelocyte leukemia), MOLT-4 (acute lymphoblastic leukemia), HeLa (cervix cancer), Caki-2 (kidney cancer), T98G (glioblastoma), and HT1080 (fibrosarcoma).

Oligonucleotide microarray. The oligonucleotide microarray was performed using a human oligo chip (CMRC-GT, Seoul, Korea) containing 22,740 oligonucleotide probes (70 bases) in a reference design. The test samples, 60 cancer cell lines RNA, were labeled with Cy5 and individually co-hybridized with the Cy3-labeled the Yonsei reference RNA (CMRC, Seoul, Korea). One hundred micrograms of the total RNA of each sample was used. The RNA was mixed with oligo-dT primer (Genotech, Daejun, Korea) and incubated at 65˚C for 10 min. Added SuperScript II (Invitrogen, USA), 5X first strand buffer, 100 mM DTT, low-dT/dNTP mix and Cy3- or Cy5-dUTP to RNA/oligo-dT mixture and reverse transcription was performed at 42˚C for 2 h. The residual RNA was hydrolyzed by incubation at 65˚C for 30 min in 0.1 M NaOH solution. The reaction was neutralized with same quantity of 0.1 M HCl. The Cy3 and Cy5 labeled probes were purified using a QIAquick PCR Purification Kit (Qiagen, Valencia, CA, USA). The purified probes were combined and mixed with Human Cot-1 DNA (Invitrogen), yeast tRNA (Invitrogen) and poly(A) RNA (Sigma). The final probe was concentrated using a Microcon YM-30 column (Millipore) and then denatured at 100˚C for 2 min. The oligonucleotide microarrays were pre-hybridized in 5× sodium chloride/sodium citrate buffer (SSC), 0.1% sodium dodesyl sulfate (SDS), and 10 mg/ml BSA at 42˚C for 1 h prior to probe application. The probe was hybridized in 30% formamide, 5X SSC and 0.1% SDS at 42˚C for 16 h. Following hybridization, the arrays were washed in 2× SSC with 0.1% SDS, 1× SSC with 0.1% SDS, 0.2× SSC, and 0.05× SSC, sequentially washed for 2 min each and then spun dried at 500 ×g. The fluorescence signals on the microarrays were acquired using a GenePix 4000B scanner (Axon Instruments, Foster City, CA, USA). The scanned images were processed using GenePix Pro 4.0 software (Axon Instruments).

Data pre-processing of microarray data. Raw Cy3/Cy5 data were $\log_2$-transformed. Systemic errors were corrected by normalization using intensity dependent, within-print tip normalization based on the Lowess function. Hierarchical clustering analysis was performed with Cluster software and the resulting dendrogram was visualized using TreeView software (http://rana.lbl.gov/EisenSoftware.htm). Cluster analysis was performed to organize the microarray data so that the underlying structures could be recognized and explored. The annotation of the selected genes was performed using the Database for Annotation, Visualization and Integrated Discovery (DAVID) (http://apps1.niaid.nih.gov/david) and Stanford Online Universal Resource for Clones and Expressed sequence tags (SOURCE) (http://source.stanford.edu/cgi-bin/source/sourceSearch).

Results

The effect of ERK inhibition in colorectal cancer cells. HCT116 and HT29 cells were treated with increasing amounts of U0126. Lysates were subjected to immunoblotting with antibodies specific for the indicated proteins as previously mentioned. The western blot analysis revealed that increasing amounts of U0126 resulted in the inhibition of pERK in both cell lines, but higher concentrations of U0126 were required for HT29 cells. In HCT116 cells, 1 μM U0126 resulted in complete disappearance of the pERK protein band, whereas in HT29 cells, 10 μM U0126 resulted in complete disappearance of the pERK protein band (Figure 1A). A time-dependent effect of U0126 on pERK is shown in Figure 1B.

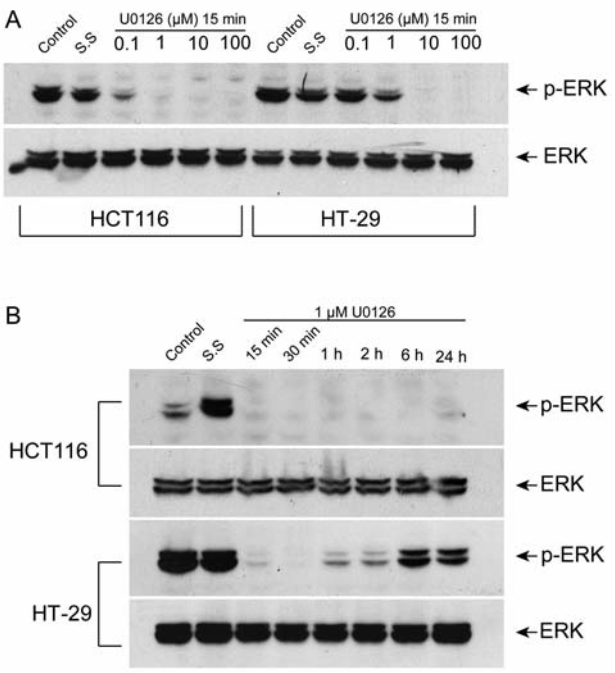

Figure 1. *A: Increasing amounts of the inhibitor U0126 resulted in the inhibition of pERK in both cell lines, but higher concentrations of U0126 were required in HT29 cells. In HCT116 cells, 1 μM U0126 resulted in complete disappearance of the pERK protein band, whereas in HT29 cells, 10 μM U0126 resulted in complete disappearance of the pERK protein band. B: A time-dependent effect of U0126 on pERK is shown.*

After treatment of the cells with 1 μM U0126, western blots were performed at 15 min, 30 min, 1 h, 2 h, 6 h, and 24 h. We observed that U0126 treatment inhibited pERK at 15 min in both cell lines. The effect of inhibition was maintained throughout 24 h in HCT116 cells, whereas it was limited to 6 h in HT29 cells. The protein bands of pERK re-appeared after 6 h in HT29 cells.

FACS plots of ERK inhibition. Figure 2 shows the FACS plots of phosphorylation of ERK in cells treated with U0126. In HCT116 cells, the U0126-mediated decrease in pERK after U0126 treatment was as follows: 55.5% at 0.1 μM, 34.4% at 1μM, 26.7% at 10 μ, and 26.0% at 100 μM (Figure 2A). Similarly, in HT29 cells, pERK decreased with increasing concentrations of U0126; the U0126-mediated decrease in pERK was as follows: 59.1% at 0.1 μM, 52.8% at 1 μM, 24.8% at 10 μM, and 18.8% at 100 μM (Figure 2B). Figures 2C shows pERK inhibition in a time-dependent manner in the two cell lines. FACS analysis was performed at 15 min, 30 min, 1 h, 2 h, 6 h, and 24 h. Following U0126 treatment of HCT116 cells, the pERK level was the lowest (11.0%) at 30 min, then increased to 22.2% at 1 h, 21.6% at 2h, 19.8% at 6 h, and 34.7% at 24 h in HCT116 cells. In HT29 cells, the pERK level was

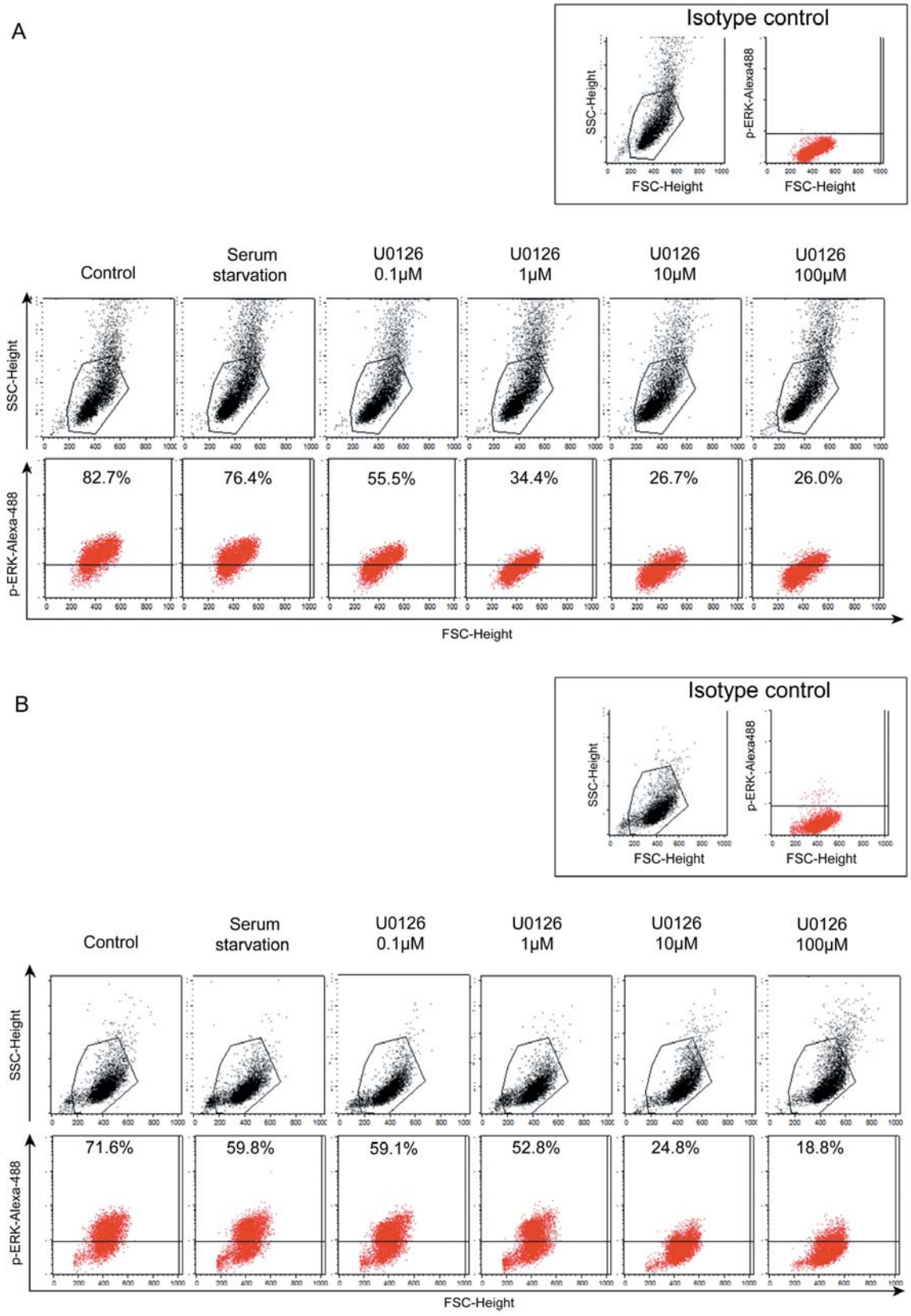

Figure 2. *continued*

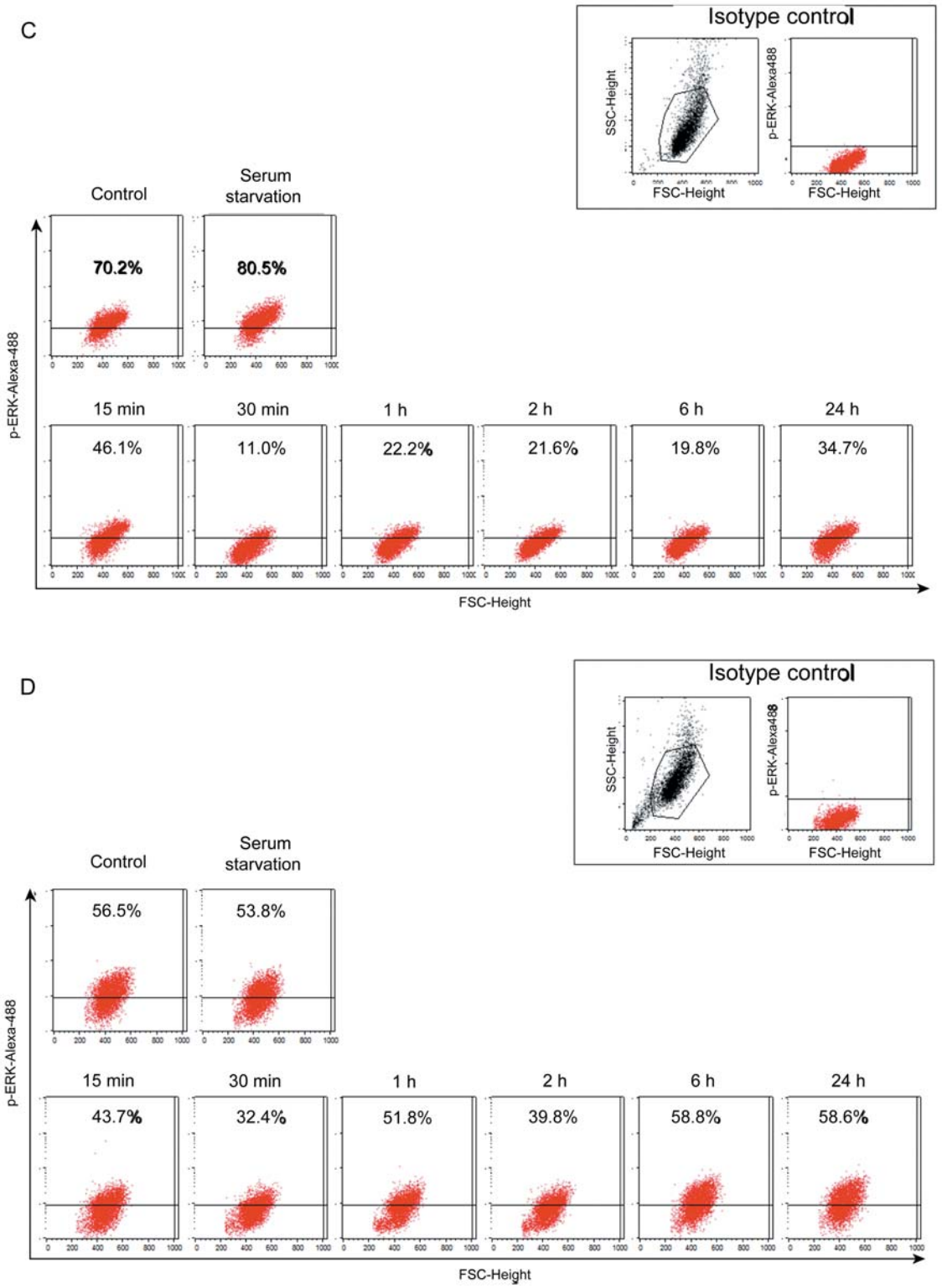

Figure 2. *Fluorescence-activated cell sorting (FACS) plots of phosphorylation of ERK in cells treated with U0126. A: In HCT116 cells, the U0126-mediated decrease in pERK is shown as a percentage. B: In HT29 cells, pERK decreased with increasing concentrations of U0126; the U0126-mediated decrease in pERK is shown as a percentage. C: Following U0126 treatment of HCT116 cells, the pERK level was the lowest (11.0%) at 30 min, then increased to 34.7% at 24 h in HCT116 cells. D: In HT29 cells, the pERK level was the lowest (32.4%) at 30 min of U0126 treatment, then increased to 58.6% at 24 h. SSC, Side scatter; FSC, forward scatter.*

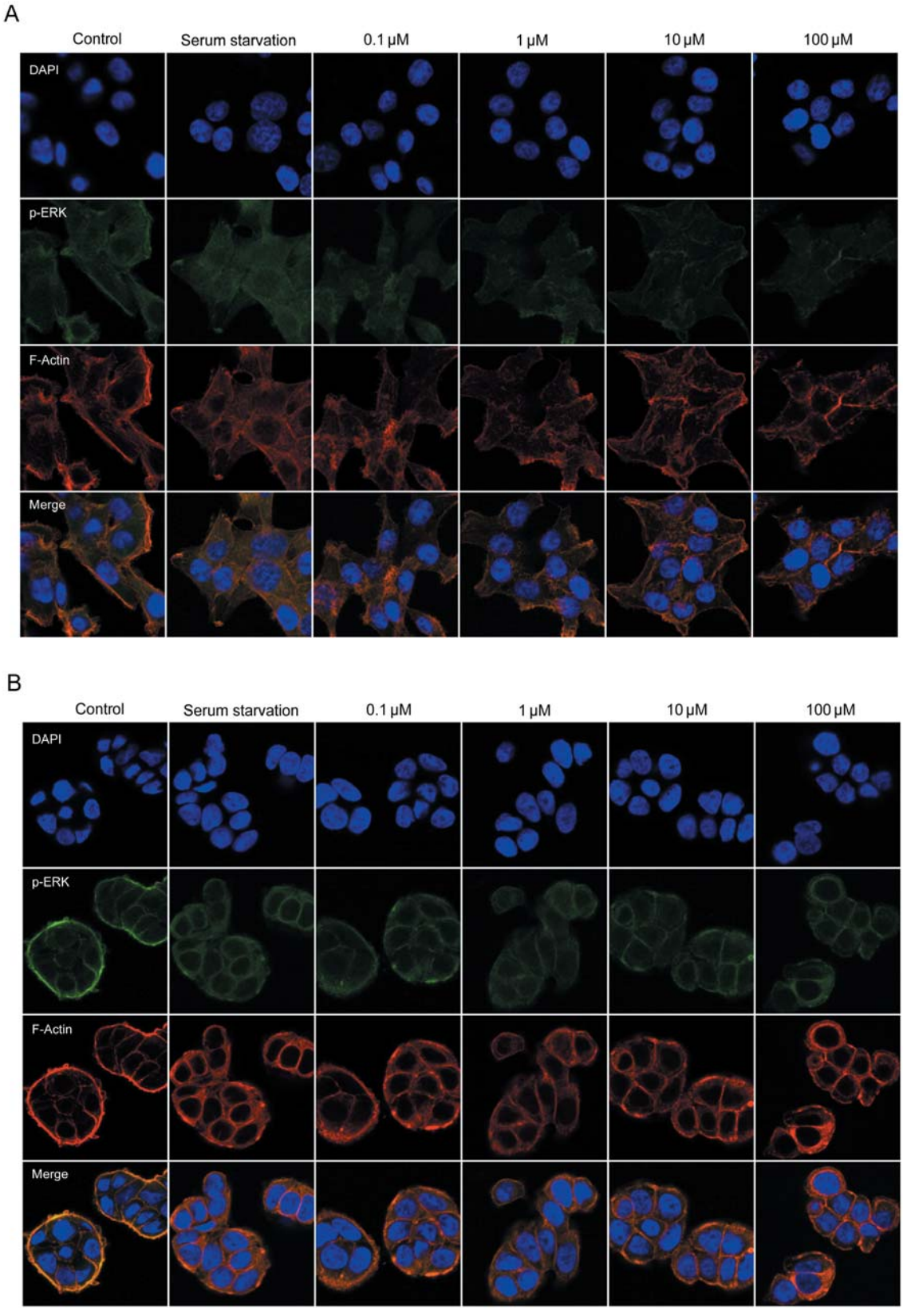

Figure 3. *continued*

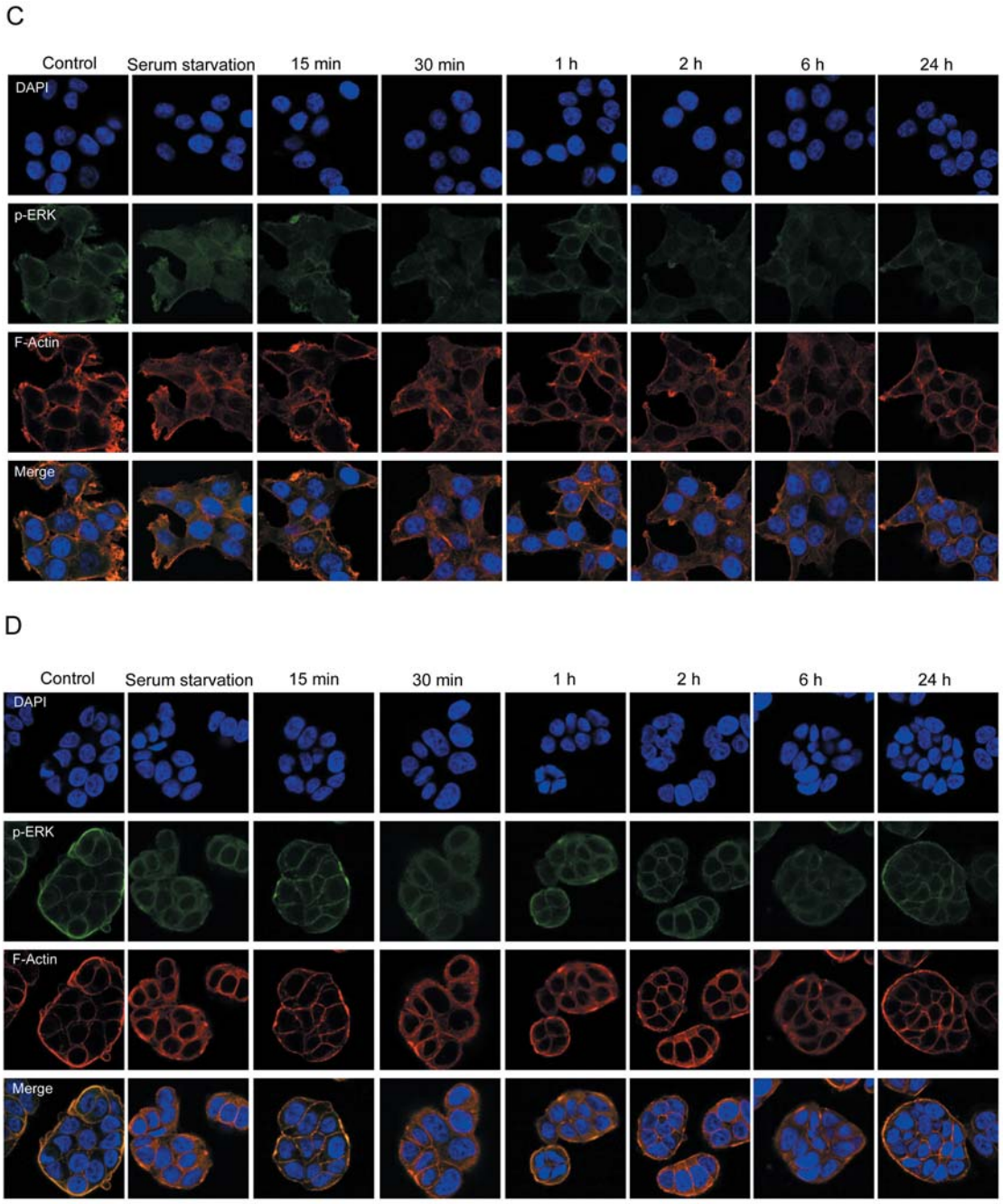

Figure 3. *A: Immunofluorescence staining was performed to evaluate the phosphorylation status of ERK in the two cell lines. In HCT116 cells, the staining intensity of the immunofluorescent dye decreased as the concentration of U0126 increased from 0.1 μM to 100 μM. B: In HT29 cells, the staining intensity of the immunofluorescent dye also decreased as the concentration of U0126 increased from 0.1 μM to 100 μM. C: Time-dependent inhibition of pERK by immunofluorescence staining is shown for HCT116 cells. D: Time-dependent inhibition of pERK by immunofluorescence staining is shown for HT29 cells.*

the lowest (32.4%) at 30 min of U0126 treatment, then increased to 41.8% at 1 h, 39.8% at 2h, 58.8% at 6 h, and 58.6 % at 24 h (Figure 2D). It is noteworthy that U0126 inhibited phosphorylation of ERK in HCT116 cells more profoundly than in HT29 cells.

Immunofluorescence staining of ERK inhibition. Immunofluorescence staining was performed to evaluate the phosphorylation status of ERK in the two cells. In HCT116 cells, the staining intensity of the immunofluorescent dye decreased as the concentration of U0126 increased from 0.1 μM

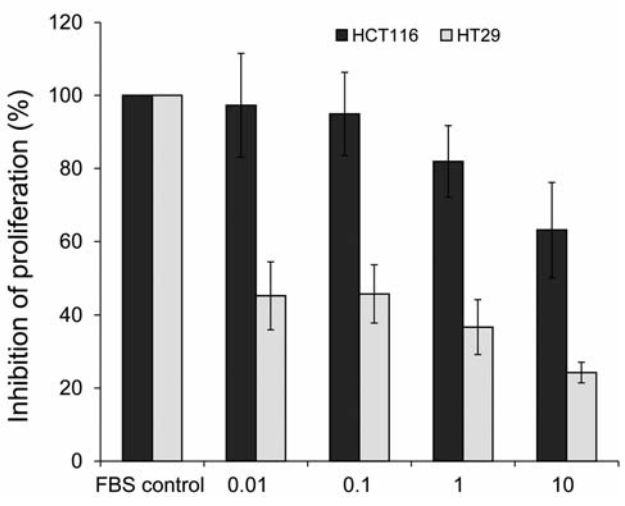

Figure 4. *Cell proliferation assay was performed in the two cell lines on treatment with increasing doses of U0126 from 0.01μM to 10 μM. Results are the mean±standard deviation of three independent experiments performed in duplicate.*

to 100 μM. This finding was also consistent with in HT29 cells (Figure 3A, B). Next, we analyzed the time-dependent inhibition of pERK by immunofluorescence staining. The effect of the inhibiting pERK by 10 μM U0126 is represented as a decrease in immunofluorescent staining of pERK over time in HCT116 cells and HT29 cells (Figure 3C, 3D). These results are in accordance with the interpretation of the FACS plots.

ERK is more sensitively inhibited in HCT116 cells. A cell proliferation assay was performed in the two cell lines after treatment with increasing dose of U0126 from 0.01 μM to 10 μM (Figure 4). The proliferation was markedly reduced in HT29 cells from 0.01 μM of U0126, whereas HCT116 cells did not show a significant decrease. This result is contrary to the finding on previous western blots, FACS plots and immunofluorescence staining data, where the phosphorylation of ERK was more sensitively inhibited in HCT116 cells.

Combination of cytochrome P1A2 inhibitor enhances sensitivity to U0126. To identify mechanisms of heterogeneous sensitivity to U0126, we conducted microarray expression profiling of both cells. We sought which genes were differentially-regulated in the two cells (unpaired *t*-test, $p<0.05$). This analysis showed that *CYP1A2* was most up-regulated in HT29 cells compared to HCT116 cells (HCT116/HT29 $\log_2$ ratio=2.99) (Figure 5A). We hypothesized that CYP1A2 overexpression and activation might promote resistance to U0126 in HT29 cells. We further examined whether inhibition of CYP1A2 resulted in U0126 sensitivity (Figure 5B). We treated HT29 cells with α-naphthoflavone (α-NF) at 20 μM in combination with U0126 treatment and observed that HT29 cells became more sensitive at 1 μM of U0126. Combination of furanfylline (FF) 10 uM and U0126 resulted in the similar findings: p-ERK was effectively inhibited at 1 μM of U0126. We next sought to determine the quantitative inhibition of pERK by phospho-flow cytometry (Figure 5C). Although it resulted in inhibition of pERK, the inhibition of pERK was statistically significant when U0126 was combined with FF rather than α-NF.

Discussion

There are numerous mutations in colon cancer cells which represent the heterogeneity of initial response to therapy. We investigated the mechanisms of heterogeneous response to an MEK/ERK inhibitor in *KRAS*- and *BRAF*-mutant colorectal cancer cells. HCT116 cells are *KRAS*- and *PIK3CA*-mutant with *KRAS* as a driver oncogene, whereas HT29 cells are BRAF-mutant and *PIK3CA*-mutant with *BRAF* as a driver oncogene. In addition, HT29 cells had high expression of CYP1A1 and 1A2 which could be inhibited by a CYP inhibitor compared to HCT116 cells. We observed synergistic inhibitory effects of phosphorylated ERK combining a CYP inhibitor with an MEK/ERK inhibitor, U0126, in HT29 cells. Our results indicate that patient responses to ERK inhibitors may rely on both the mutational status of driver oncogenes and efficiency of intracellular drug metabolism in cancer cells. CYP1A1 and 1A2 are the main cytochrome *P450* enzymes that are responsible for drug metabolism. Drug metabolism in targeted agents has not been emphasized, but inter-individual variations of drug-metabolizing capacity both in germline and somatic cells complicate a uniform treatment response. Such differences may be important determinants of drug resistance which leads to a reduction in intracellular drug concentrations in somatic cancer cells. In our study, the inhibition of CYP1A1 by α-NF and FF resulted in a dramatic inhibition of phosphorylated ERK in HT29 cells. It is feasible that concomitant administration of targeted agents with agents that inhibit CYP1A1 will enhance drug efficacy. In a recent study, ketoconazole, both a broad-spectrum imidazole antifungal agent and a strong inhibitor of CYP3A, was concomitantly administered with bortezomib in patients with solid tumors. Since bortezomib undergoes oxidative biotransformation *via* CYP3A4, concomitant administration of ketoconazole produced a 35% increase in bortezomib exposure (11). Future investigations of combining CYP1A1 inhibitor with ERK inhibitor in patients colon cancer patients with BRAF mutation and KRAS mutation will be necessary with regards to efficacy and safety. In clinical settings, we tend to seek for single-driver mutations that activate oncogenic signaling in advanced solid tumors. However, diverse mutations can exist in the same tumor which arise from different clonal populations. This hinders effective inhibition of oncogenic signaling pathways and thus blocking a single

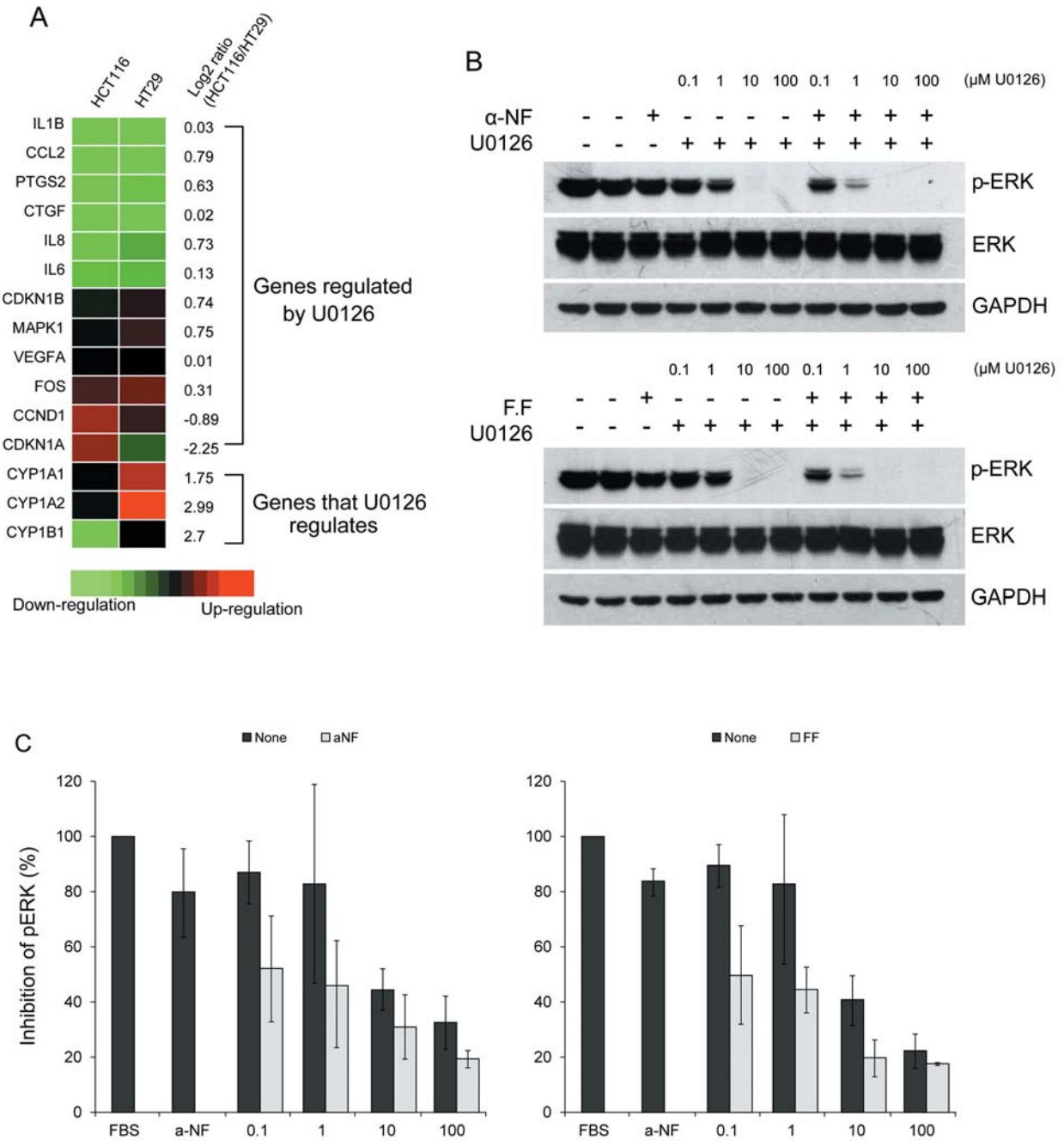

Figure 5. *A: Microarray expression profiling of both cell lines showed that CYP1A2 was most upregulated in HT29 cells compared to HCT116 cells (HCT116/HT29 log2 ratio=2.99). B: Treatment with α-naphthoflavone (α-NF) at 20 μM in combination with U0126 treatment showed that HT29 cells became more sensitive at 1 μM of U0126. Combination of furanfylline (FF) at 10μM and U0126 resulted in similar findings: p-ERK was effectively inhibited at 1 μM of U0126. C: Quantitative inhibition of pERK by phospho-flow cytometry was performed. Although it resulted in inhibition of pERK, the inhibition of pERK was statistically significant when U0126 was combined with FF rather than α-NF. α-NF; α-naphtoflavone, FF; furanfylline.*

downstream target may not be sufficient to inhibit tumor growth. In addition, each of these pathways contains multiple genes, and there are numerous combinations of mutations that can perturb a pathway important for cancer (12, 13). Another important issue to take into account is the presence of negative feedback loops. Recently, it was found that BRAF inhibition rapidly causes a feedback activation of EGFR, which supports continued proliferation in the presence of BRAF inhibition (14).

This provides a rationale for combining BRAF and EGFR inhibitors in *BRAF*-mutant colorectal cancer, which confer a poor clinical outcome. In this aspect, a dual-targeted or multi-targeted strategy may therefore be more efficient, but the number of possible combinations of these agents seems endless and needs to be confirmed in clinical trials for safety. As high-throughput technologies have been recently developed to characterize genetic alterations, many genomic abnormalities have been identified in colon cancer (15). Whole-exome sequencing and integrative analysis of genomic data provide us with further insights into the novel pathways that are de-regulated in colon cancer. This means finding more and more novel targets for inhibition and these should be validated in clinical trials. Clinical trials should also validate not only drug efficacy and safety, but also pharmacokinetics. In summary, our results provide a rationale for combining MEK/ERK inhibitor and cytochrome P inhibitor in *BRAF*-mutant colorectal cancer with high expression of cytochrome Ps. Selecting proper driver oncogenes and understanding the mechanisms of intrinsic drug resistance are essential in development of more effective targeted therapies and new therapeutic combinations.

Financial Disclosure and Conflicts of Interest

None declared.

Acknowledgements

This research was supported by basic Science Research Program through the National Research Foundation of Korea (NRF) funded by the Ministry of Education, Science and Technology (2010-0010667).

References

1 Blume-Jensen P and Hunter T: Oncogenic kinase signaling. Nature *411*: 355-365, 2001.

2 Lipson D, Capelletti M, Yelensky R, Otto G, Parker A, Jarosz M, Curran JA, Balasubramanian S, Bloom T, Brennan KW, Donahue A, Downing SR, Frampton GM, Garcia L, Juhn F, Mitchell KC, White E, White J, Zwirko Z, Peretz T, Nechushtan H, Soussan-Gutman L, Kim J, Sasaki H, Kim HR, Park SI, Ercan D, Sheehan CE, Ross JS, Cronin MT, Janne PA and Stephens PJ: Identification of new ALK and RET gene fusions from colorectal and lung cancer biopsies. Nature Med *18*: 382-384, 2011

3 Thomas RK, Baker AC, Debiasi RM, Winckler W, Laframboise T, Lin WM, Wang M, Feng W, Zander T, MacConaill L, Lee JC, Nicoletti R, Hatton C, Goyette M, Girard L, Majmudar K, Ziaugra L, Wong KK, Gabriel S, Beroukhim R, Peyton M, Barretina J, Dutt A, Emery C, Greulich H, Shah K, Sasaki H, Gazdar A, Minna J, Armstrong SA, Mellinghoff IK, Hodi FS, Dranoff G, Mischel PS, Cloughesy TF, Nelson SF, Liau LM, Mertz K, Rubin MA, Moch H, Loda M, Catalona W, Fletcher J, Signoretti S, Kaye F, Anderson KC, Demetri GD, Dummer R, Wagner S, Herlyn M, Sellers WR, Meyerson M and Garraway LA: High-throughput oncogene mutation profiling in human cancer. Nat Genet *39*: 347-351, 2007

4 Parsons DW, Wang TL, Samuels Y, Bardelli A, Cummins JM, DeLong L, Silliman N, Ptak J, Szabo S, Willson JK, Markowitz S, Kinzler KW, Vogelstein B, Lengauer C and Velculescu VE: Colorectal cancer: Mutations in a signaling pathway. Nature *436*: 792, 2005.

5 Yu K, Toral-Barza L, Shi C, Zhang WG and Zask A: Response and determinants of cancer cell susceptibility to PI3K inhibitors: Combined targeting of PI3K and MEK1 as an effective anticancer strategy. Cancer Biol Ther *7*: 307-315, 2008.

6 Engelman JA, Chen L, Tan X, Crosby K, Guimaraes AR, Upadhyay R, Maira M, McNamara K, Perera SA, Song Y, Chirieac LR, Kaur R, Lightbown A, Simendinger J, Li T, Padera RF, Garcia-Echeverria C, Weissleder R, Mahmood U, Cantley LC and Wong KK: Effective use of PI3K and MEK inhibitors to treat mutant *KRAS* G12D and *PIK3CA* H1047R murine lung cancers. Nat Med *14*: 1351-1356, 2008.

7 Sebolt-Leopold JS, Dudley DT, Herrera R, Van Becelaere K, Wiland A, Gowan RC, Tecle H, Barrett SD, Bridges A, Przybranowski S, Leopold WR and Salitiel AR: Blockade of the MAP kinase pathway suppresses growth of colon tumors *in vivo*. Nat Med *5*: 810-816, 1999.

8 Yeh TC, Marsh V, Bernat BA, Ballard J, Colwell H, Evans RJ, Parry J, Smith D, Brandhuber BJ, Gross S, Marlow A, Hurley B, Lyssikatos J, Lee PA, Winkler JD, Koch K and Wallace E: Biological characterization of ARRY-142886 (AZD6244), a potent, highly selective mitogen-activated protein kinase kinase 1/2 inhibitor. Clin Cancer Res *13*: 1576-1783, 2007.

9 Solit DB, Garraway LA, Pratilas CA, Sawai A, Getz G, Basso A, Ye Q, Lobo JM, She Y, Osman I, Golub TR, Sebolt-Leopold J, Sellers WR and Rosen N: *BRAF* mutation predicts sensitivity to MEK inhibition. Nature *439*: 358-362, 2006.

10 Androutsopoulos VP, Tsatsakis AM and Spandidios DA: Cytochrome P450 CYP1A1: Wider roles in cancer progression and prevention. BMC Cancer *9*: 187, 2009.

11 Venkatakrishnan K, Rader M, Ramanathan RK, Ramalingam S, Chen E, Riordan W, Trepicchio W, Cooper M, Karol M, Moltke L, Neuwirth R, Egorin M and Chatta G: Effect of the CYP3A inhibitor ketoconazole on the pharmacokinetics and pharmaco-dynamics of bortezomib in patients with advanced solid tumors: a prospective, multicenter, open-label, randomized, two-way crossover drug-drug interaction study. Clin Ther *31*: 2444-2458, 2009.

12 Vandin F, Upfal E and Raphael BJ: *De novo* discovery of mutated driver pathways in cancer. Genome Res *21*: 2303-2312, 2011.

13 Yap TA, Gerlinger M, Futreal PA, Pusztai L and Swanton C: Intratumor heterogeneity: seeing the wood for the trees. Sci Transl Med Mar 28, 2012.

14 Prahallad A, Sun C, Huang S, Di Nicolantonio F, Salazar R, Zecchin D, Beijersbergen RL, Bardelli A and Bernards R: Unresponsiveness of colon cancer to BRAF(V600E) inhibition through feedback activation of EGFR. Nature *483*: 100-104, 2012.

15 The Cancer Genome Atlas Network. Comprehensive molecular characterization of human colon and rectal cancer. Nature *487*: 330-337, 2012.

Received May 2, 2013
Revised May 22, 2013
Accepted May 23, 2013